Numerical Studies of Reacting Flows over Flat Walls with Fuel Injection*
(Part 1, Velocity Anomaly and Hydrodynamic Instability)

Xiao WANG**, Toyohiko SUZUKI**,
Yoshitaka OCHIAI** and Shigeharu OHYAGI***

A computational study is performed on a chemically reacting laminar boundary layer over a porous horizontal wall with a diffusion flame. The generation of counter-rotating vortices along the flame sheet is observed. Our attention is focused on i) local acceleration, which induces an anomaly in the velocity distributions across the flat plate boundary layer, and ii) the origin of hydrodynamic instability, which may disturb and wrinkle the flame downstream. Results show that when reaction exothermicity is taken into account in the numerical simulation, both the aerodynamic structures and the mass transfer of the chemical species change significantly, especially in the region near the front edge of the burner. Counter-rotating vortices are generated along the flame sheet and are expected to induce hydrodynamic instability. A high pressure zone in front of the leading flame edge and local acceleration are numerically simulated in agreement with experimental observation. Buoyancy plays a negligible role in the behavior of flow and combustion in regions upstream of the burner.

Key Words: Boundary Layers, Two-dimensional, Laminar Flow, Combustion, Numerical Simulation

1. Introduction

Flows of chemically reacting boundary layers are of interest in many practical problems involving the combustion of solid and liquid fuels, such as fires over structures and liquid pools, catalytic reactors in chemical industries and hybrid propulsion devices. A simple physical description of a reacting boundary layer flow is that gaseous or gasified fuel is diffused and convected from the wall surface into the oxidizing boundary layer and so does the oxidant from the main stream. Chemical reactions occur within the boundary layer, and the heat of reaction released is transferred to the plate surface by diffusion and convection. The stability and intensity of the combustion are thus closely related to the aerodynamic and thermal features of the boundary layer flow. Hence, the coupling of combustion and fluid dynamics has to be clarified to enable the physical understanding of these problems and to actively control them. Many experimental and numerical studies have been conducted over several decades and some share one facet of this study.

Using boundary layer theory, Emmons[1] studied the burning rate of condensed fuel in an oxidizing stream and obtained profiles of velocity, temperature and concentration in the boundary layer flow. Hirano et al.[2],[3] experimentally measured the gas velocity and temperature profiles over a wall with fuel gas injection and over the surface of a liquid fuel. Flow acceleration was observed near the blue-flame zone downstream of the leading flame edge. Zhou and Fernandez-Pello[4] studied the effects of main stream velocity, turbulence and buoyancy on the combustion of a solid fuel in a flat plate boundary layer flow and showed that main stream velocity influenced the processes of heat and mass transfer within the layer and hence the burning rate of the fuel plate. With the same boundary layer approximation, Lavid and Berlad[5] carried out a theoretical study on a chemically reacting laminar boundary layer flow over a horizontal flat plate and showed that the local acceleration is caused mainly by buoyancy, which acted effectively to produce a streamwise favorable pres-

* Received 5th September, 1996
** Department of Mechanical Engineering, Tottori University, Tottori 680, Japan
*** Department of Mechanical Engineering, Saitama University, Urawa 338, Japan

sure gradient. Mori et al.[6] reported experimental and numerical results for profiles of velocity, temperature and chemical species within a boundary layer flow and also observed a streamwise velocity overshoot. In absence of buoyancy, however, Trevino[7] observed a high pressure zone upstream of the leading flame edge and a streamwise velocity overshoot in a problem of igniting a combustible mixture flowing over an inert flat plate. Chen and T'ien[8] presented a theoretical model of a laminar diffusion flame at the leading edge of a fuel plate in a forced convective flow. Using finite-rate Arrhenius kinetics, they investigated the flow and flame structures, especially in the leading edge at different Damköhler numbers.

In spite of many studies carried out on this kind of reacting boundary layer flow, there still remain some problems that have not yet been completely clarified, such as mechanisms of the velocity overshoot when a flame zone is present and flame instability downstream of the leading flame. The velocity overshoot cannot be predicted by classical self-similar boundary layer theory. In this paper, the effect of baroclinic torque ($\nabla\rho\times\nabla p/\rho^2$) was examined, which is mainly responsible for the generation of counter-rotating vortices along the flame sheet. The movement and development of these vortices are closely related to the local acceleration and the hydrodynamic instability; two-dimensional compressible Navier-Stokes equations are numerically integrated by a finite difference method. Attention is focused on the effects of reaction exothermicity, free stream velocity and buoyancy due to variable density, which may alter development of the boundary layer flow in combination with fuel injection, flame instability, processes of mass transfer and thermal conduction.

2. Physical Model and Governing Equations

The omputational domain shown in Fig. 1 is 350 mm long and 100 mm wide. Fuel is injected from a porous plate within the region from $x=40$ mm to 110 mm with uniform velocity, forming a burner of 70 mm long. The chemical reaction occurs within the boundary layer; a diffusion flame is formed and developed by flowing a main air stream containing both oxygen and nitrogen over the horizontal flat plate. The governing partially differential equations of mass, momentum, energy and chemical species are deduced for two-dimensional laminar reacting flows with the following assumptions:

a) the flow is two-dimensional and laminar;

b) a one-step, irreversible chemical reaction takes place with reaction heat release and a flame-sheet model is available

$$\nu_{fu}[F]+\nu_{ox}[O]\longrightarrow\nu_{pr}[P]+\text{heat}; \tag{1}$$

c) the reactants and product are perfect gases with equal and constant specific heats and equal diffusion coefficients;

d) the Soret and Dufour effects, along with pressure diffusion and pressure work, can be neglected;

d) the Lewis number is unity, and

e) diffusion coefficients are temperature-dependent, obeying the law given by Strehlow[9]

$$\mu\propto T^{0.7},\quad D\propto T^{1.7},\quad \alpha\propto T^{1.7}.$$

Although the use of a one-step overall reaction and the flame-sheet model is inadequate in predicting the details of a diffusion flame and its extinction and blow-off, it is sufficient to predict the behavior of the overall structure of the flame and its interaction with a flowfield because of the reaction heat release. For the problem concerned, as a significant temperature change occurs due to reaction heat release, it is important to deal with the temperature-dependent diffusion coefficients. According to the above assumptions, the governing equations are written as follows:

Continuity equation

$$\frac{\partial\rho}{\partial t}+\frac{\partial(\rho u)}{\partial x}+\frac{\partial(\rho v)}{\partial y}=0, \tag{2}$$

Momentum equations

$$\frac{\partial(\rho u)}{\partial t}+\frac{\partial(\rho uu)}{\partial x}+\frac{\partial(\rho uv)}{\partial y}=-\frac{\partial p}{\partial x}+\frac{\partial}{\partial x}\mu\left[2\frac{\partial u}{\partial x}-\frac{2}{3}\left(\frac{\partial u}{\partial x}+\frac{\partial v}{\partial y}\right)\right]+\frac{\partial}{\partial y}\left[\mu\left(\frac{\partial u}{\partial y}+\frac{\partial v}{\partial x}\right)\right], \tag{3}$$

$$\frac{\partial(\rho v)}{\partial t}+\frac{\partial(\rho vu)}{\partial x}+\frac{\partial(\rho vv)}{\partial y}=-\frac{\partial p}{\partial y}+\rho g\beta(T-T_\infty)+\frac{\partial}{\partial x}\left[\mu\left(\frac{\partial u}{\partial y}+\frac{\partial v}{\partial x}\right)\right]+\frac{\partial}{\partial y}\mu\left[2\frac{\partial v}{\partial y}-\frac{2}{3}\left(\frac{\partial u}{\partial x}+\frac{\partial v}{\partial y}\right)\right], \tag{4}$$

Energy equations

$$C_p\left[\frac{\partial(\rho T)}{\partial t}+\frac{\partial(\rho Tu)}{\partial x}+\frac{\partial(\rho Tv)}{\partial y}\right]=\frac{\partial}{\partial x}\left(\lambda\frac{\partial T}{\partial x}\right)+\frac{\partial}{\partial y}\left(\lambda\frac{\partial T}{\partial y}\right)+Qw_{fu}, \tag{5}$$

Chemical species equations

$$\frac{\partial(\rho Y_i)}{\partial t}+\frac{\partial(\rho Y_iu)}{\partial x}+\frac{\partial(\rho Y_iv)}{\partial y}=\frac{\partial}{\partial x}\left(\rho D_i\frac{\partial Y_i}{\partial x}\right)+\frac{\partial}{\partial y}\left(\rho D_i\frac{\partial Y_i}{\partial y}\right)+w_i, \tag{6}$$

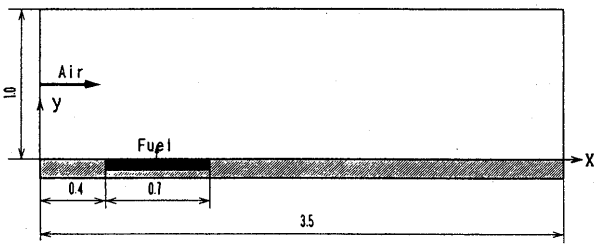

Fig. 1 Physical model for the computation

$i=CH_4, O_2, N_2$, Product,

where ρ, u, v, p, T and Y_i are the density, velocity components in both the x and y-directions, pressure, temperature and mass fraction of ith chemical species for the mixture gas, respectively. The term $\beta \equiv -1/\rho(\partial\rho/\partial T)|_p$ is the coefficient of thermal expansion. The equation of thermodynamic state is

$$\rho=\frac{p}{RT}, \tag{7}$$

where R is the gas constant of the mixture estimated by

$$R=\sum_{i=1}^{n}\frac{Y_i}{W_i}R_u. \tag{8}$$

The term R_u is the universal gas constant and W_i is the molecular weight for the ith species. Based on assumptions (b) and (d), the behavior of the chemical reaction and its coupling with fluid dynamics can be obtained by solving a conservation equation for the coupling function f, instead of those for energy and the respective species. The height of the computational domain is chosen as the characteristic length, and the state of the main air stream at $T_\infty=$ 300 K and one atmospheric pressure is specified as the reference to normalize the above governing equations. The dimensionless equations are:

Continuity equation

$$\frac{\partial\rho^*}{\partial t^*}+\frac{\partial(\rho^* u^*)}{\partial x^*}+\frac{\partial(\rho^* v^*)}{\partial y^*}=0, \tag{9}$$

Momentum equations

$$\frac{\partial(\rho^* u^*)}{\partial t^*}+\frac{\partial(\rho^* u^* u^*)}{\partial x^*}+\frac{\partial(\rho^* u^* v^*)}{\partial y^*}$$
$$=-\frac{\partial p^*}{\partial x^*}+\frac{\partial}{\partial x^*}\frac{\mu^*}{Re}\left[2\frac{\partial u^*}{\partial x^*}-\frac{2}{3}\left(\frac{\partial u^*}{\partial x^*}+\frac{\partial v^*}{\partial y^*}\right)\right]$$
$$+\frac{\partial}{\partial y^*}\left[\frac{\mu^*}{Re}\left(\frac{\partial u^*}{\partial y^*}+\frac{\partial v^*}{\partial x^*}\right)\right], \tag{10}$$

$$\frac{\partial(\rho^* v^*)}{\partial t^*}+\frac{\partial(\rho^* v^* u^*)}{\partial x^*}+\frac{\partial(\rho^* v^* v^*)}{\partial y^*}$$
$$=-\frac{\partial p^*}{\partial y^*}+\frac{Gr}{Re^2}\rho^*\frac{T^*-1.0}{T_f^*-1.0}$$
$$+\frac{\partial}{\partial x^*}\left[\frac{\mu^*}{Re}\left(\frac{\partial u^*}{\partial y^*}+\frac{\partial v^*}{\partial x^*}\right)\right]$$
$$+\frac{\partial}{\partial y^*}\frac{\mu^*}{Re}\left[2\frac{\partial v^*}{\partial y^*}-\frac{2}{3}\left(\frac{\partial u^*}{\partial x^*}+\frac{\partial v^*}{\partial y^*}\right)\right], \tag{11}$$

Coupling function equation

$$\frac{\partial(\rho^* f)}{\partial t^*}+\frac{\partial(\rho^* f u^*)}{\partial x^*}+\frac{\partial(\rho^* f v^*)}{\partial y^*}$$
$$=\frac{\partial}{\partial x^*}\left(\frac{\rho^* D^*}{Re Pr}\frac{\partial f}{\partial x^*}\right)+\frac{\partial}{\partial y^*}\left(\frac{\rho^* D^*}{Re Pr}\frac{\partial f}{\partial y^*}\right). \tag{12}$$

According to the flame sheet model and the definition of the coupling function, the mass fraction of each species and the temperature can be obtained by:

$$\begin{aligned}
&0<f\le f_{st}:\\
&Y_{fu}=0,\\
&Y_{ox}=(1-f/f_{st})\,Y_{ox,inlet},\\
&T^*=1+Q^* f_{st}(1-f)/(1-f_{st});\\
&1>f>f_{st}:\\
&Y_{fu}=(f-f_{st})/(1-f_{st}),\\
&Y_{ox}=0,\\
&T^*=1+Q^* f.
\end{aligned} \tag{13}$$

The mass fractions of nitrogen and the product are obtained from

$$Y_{N_2}=Y_{N_\infty}(1-f), \tag{14}$$
$$Y_{pr}=1-(Y_{ox}+Y_{fu}+Y_{N_2}). \tag{15}$$

In the above equations, f_{st} is the stoichiometric value of the coupling function and is given by $f_{st}\equiv 1/(1+sY_{fu}/Y_{ox}|_{inlet})$. Its value is taken as 0.055 for the methane-air reaction. The dimensionless variables are defined as:

$$\begin{aligned}
&x^*=\frac{x}{H}, y^*=\frac{y}{H}, u^*=\frac{u}{U_\infty}, v^*=\frac{v}{U_\infty},\\
&T_f^*=\frac{T_f}{T_\infty}, \rho^*=\frac{\rho}{\rho_\infty}, p^*=\frac{p}{\rho_\infty U_\infty^2},\\
&\mu^*=\frac{\mu}{\mu_\infty}, D^*=\frac{D}{D_\infty}, T^*=\frac{T}{T_\infty},\\
&Q^*=\frac{Q}{C_p T_\infty}, Pr=\frac{\mu_\infty}{\rho_\infty D_\infty}, Re=\frac{\rho_\infty U_\infty H}{\mu_\infty},\\
&Gr=\frac{\beta_\infty g H^3(T_f-T_\infty)}{\nu_\infty^2},
\end{aligned} \tag{16}$$

where T_f is the adiabatic flame temperature and Q is the reaction heat release in Eq. (1). Boundary conditions are given as follows:

Inlet

$$u=U(y), v=V(y), f=0, p=p_\infty^*, \tag{17}$$

where U and V are functions determined by Blausius's results for a fully-developed laminar boundary layer flow.

Outlet

$$\frac{\partial\phi}{\partial x}=0, \quad \phi\equiv(u, v, p, f), \tag{18}$$

Upper

$$\frac{\partial\phi}{\partial y}=0, \quad v=0, \quad \phi\equiv(u, p, f), \tag{19}$$

Wall

$$\begin{aligned}
&\frac{\partial\phi}{\partial y}=0, \quad u=0, \quad v=0, \quad \phi\equiv(p, f),\\
&\frac{\partial f}{\partial y}=0, \; v=0, \quad \text{(other part of the wall)},\\
&f=1, \; v=v_w \quad \text{(on the porous wall)}.
\end{aligned} \tag{20}$$

The term v_w is the vertical injecting velocity of the fuel from the burner. Referencing Lee and T'ien's work[10] on the gas phase chemical reaction where the fuel is methane (CH_4), the value of related properties are specified: $Pr=0.714$, $L_e=1$, $Q^*=116.8$. The injecting velocity v_w is chosen as 7 cm/s corresponding to our experimental conditions at which a stable flame is steadily established on the front end of the burner. The governing equations are numerically integrated by SIMPLE procedure, and many numerical experiments have been carried out to properly specify the size of the computational domain and the

Table 1 Computed cases

Case No.	Abbre.	Re	Incom/com	Gr
Case 1	NHR/LRe	3117	Incom	0
Case 2	NHR/MRe	6234	Incom	0
Case 3	NHR/HRe	9351	Incom	0
Case 4	HR/LRe	3117	Com	0
Case 5	HR/MRe	6234	Com	0
Case 6	HR/HRe	9351	Com	0
Case 7	HR/MRe	6234	Com	2×10^7

mesh. A nonuniform mesh is adopted with grid nodes 401×146.

3. Results and Discussions

Computations were performed for many conditions from which seven typical cases have been selected. In Table 1, the selected conditions are listed. The acronyms 'NHR' and 'HR' represent chemical reactions without and with heat release; 'LRe', 'MRe' and 'HRe', the low, medium and high Reynolds numbers of the main stream; 'Incom' and 'Com', the flows without or with density variation. The acronym 'Gr' is the Grashof number involving the effect of buoyancy due to the variation in density.

3.1 Effect of density variation

To examine how the injection of fuel and reaction heat release affect flow acceleration and flame instability, comparisons are made for cases 2 and 5 at $R_e = 6234$, where Case 5 is adopted as the common case in these computations so that the extent of the influence of different parameters may be easily discerned. Profiles of the velocity u in the x-direction along the y-direction are depicted at the front in Fig. 2(a) and the rear in Fig. 2(b) of the burner for the two cases. The front end of the burner is at $x=0.4$ as shown in Fig. 1. Adjacent to the burner surface, the velocity profile is not as full as that of the developed laminar boundary layer over a flat plate, the velocity increase being suppressed near the wall. This is mainly due to vertical fuel injection from the surface of the burner, which necessarily increases the thickness of the boundary layer. For NHR, the velocity increases monotonically with the increase in y; no essential discrepancies in these profiles can be found even downstream as the chemical reaction is decoupled from the flowfield. For HR, the velocity displays a hump-shaped profile, i.e., increasing away from the

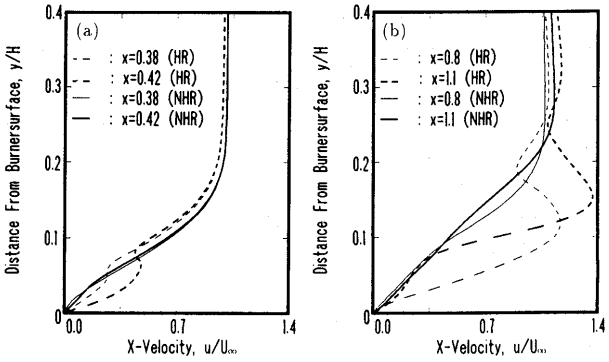

Fig. 2 Profiles of the velocity in the x-direction

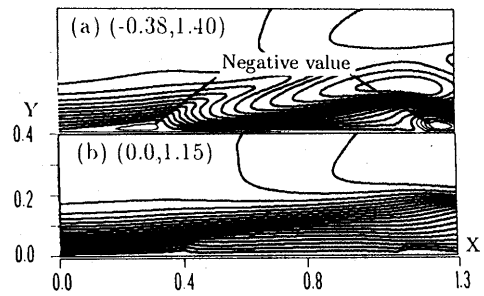

Fig. 3 Contours of the velocity in the x-direction for (a) HR and (b) NHR (data in brackets indicate maxima and minima of the contours)

burner surface, peaking near the flame sheet, going down to a valley and reaching a constant asymptotically. The peak position from the burner surface tends to become larger downstream over the burner. This local acceleration has been observed in other experiments[2),3)] and is known as the velocity overshoot when the value of the hump peak exceeds the main stream velocity as shown in Fig. 2(b). The velocity overshoot, in fact, is not limited in reacting wall boundary layer flows, and it has also been found in a counter-flowing reacting free shear layer reported by McMurtry et al.[11] in their numerical studies. The latter means that the velocity overshoot is not unique phenomenon in a reacting boundary layer over a flat plate. The recirculating zone of the flowfield is seen in Fig. 3, which shows contours of the velocity in the x-direction for HR in Fig. 3(a) and for NHR in Fig. 3(b). The bold lines represent positive value and the narrow ones, negative values. For HR, two regions of recirculating flow are found, one located close to the front end of the burner, and the other at the rear end of the burner, indicated by a negative velocity. The region of local maximum velocity is located below the flame sheet ($y<0.2$) within the fuel, and the nondimensional maximum velocity is 1.40, larger than the main stream velocity by 40%. For NHR, there also exists a slight velocity overshoot at $y \approx 0.4$ above the flame sheet, it is thought to be caused

by mass addition from the burner surface. Contours of pressure and vorticity are shown in Fig. 4 for the two cases. The negative value of pressure results from subtracting the pressure from a reference state. By comparing the pressure contours in Figs. 4(a) and 4(b), one can observe a high pressure zone located near the wall upstream of the burner for HR. The high pressure zone results in a deceleration upstream and an acceleration downstream. For NHR, a somewhat weaker high pressure zone appears vertically over the burner and is further away from the surface than that for HR. This is the reason why recirculation and acceleration are quite marked for HR. From Figs. 4(c) and 4(d), it is noted that most of the vorticity field is dominated by negative values (fluid elements rotating in clockwise direction) for NHR, but by positive vorticity in the region along the flame sheet for HR. Within the region, location of the flame sheet is indicated by a series of small circles in Fig. 4(d). To explain this observation, vorticity dynamics may be useful to study and interpret the coupling between the flow and the exothermic chemical reaction. For two-dimensional flow the vorticity equation may be written as

$$\frac{D\omega}{Dt}+\omega\nabla\cdot v=\nabla\rho\times\nabla p/\rho^2+\frac{1}{Re}\nabla\times(\nabla\cdot\tilde{\tau}), \quad (21)$$

where $\tilde{\tau}$ is the viscous stress tensor. The first term on the right-hand side is referred to as baroclinic torque; the second on the left-hand side, a change due to thermal expansion. For NHR, effects of thermal expansion and baroclinic torque may be negligible, while for HR, these two mechanisms become important to affect behavior of the flow and the flame. An illustration of the vorticity change and contours of the baroclinic torque are given in Fig. 5 for HR. Contours of Fig. 5(b) are the same vorticity field as shown in Fig. 4(d) and are simply drawn at a larger vorticity interval than Fig. 4(d) to emphasize the positive vorticity in a region along the flame sheet. Because fast kinetics is assumed herein, a flame sheet divides the flowfield into two parts: the air side over it and the fuel side under it. As shown in Fig. 5(a), the positive density gradient is normally directed outward to two sides of the flame sheet because the density is lowest there. However, the pressure gradient does not change its sign across the flame sheet and is directed toward the high pressure zone. Thus, the baroclinic torque remains positive on the air side and negative on the fuel side. On the other hand, vorticity generation occurs due to thermal expansion on the two sides of the flame sheet and remains positive because the original flow field has a predominantly negative vorticity. An overall augmentation of vorticity is generated with a positive sign on the air side, and on the fuel side, its sign depends on the predominant effect between the baroclinic torque and thermal expansion. From Fig. 5(b), a narrow strip zone is found with a positive vorticity along the flame sheet, surrounding which is the region of negative vorticity. This means that the series of vortices along the flame sheet rotates in a direction opposite the surrounding ones. Movement and development of the counter-rotating vortices certainly may disturb the flame sheet and may wrinkle the flame sheet if they become strong enough.

Profiles of the velocity v in the y-dion along y are depicted at the front end in Fig. 6(a) and the rear end in Fig. 6(b) of the burner in the two cases. For HR, the velocity profiles undulate violently and fall sharply to minima across the flame sheet. This behavior is due to thermal expansion. The highest negative

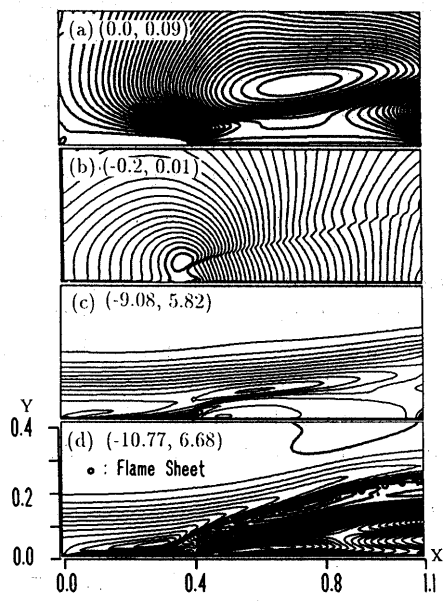

Fig. 4 Contours of pressure and vorticity: (a) pressure for NHR, (b) pressure for HR, (c) vorticity for NHR, and (d) vorticity for HR (data in brackets indicate maxima and minima of the contours)

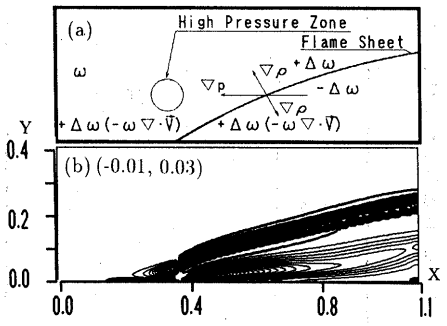

Fig. 5 (a) Illustration of changes in vorticity and (b) contours of the baroclinic torque for HR (data in brackets indicate maximum and minimum of the contours)

velocity is at $x=0.38$, and towards downstream the velocity tends to shift positively. In contrast to these, the profile changes mildly along the y-direction even across the flame sheet for NHR because not only is there no reaction heat release but also the pressure gradient is small in the y-direction as shown in Fig. 4(a). Another distinction between the two cases is that a negative velocity is present clearly only for HR near the front end of the burner (Fig. 6(a)), which changes the process of mass transfer there.

Profiles of mass fractions of the oxidizer and the fuel along the y-direction are given in Fig. 7 at the four x-direction positions and for the two cases. The location in the y-direction where the oxidizer and the fuel react chemically and are consumed completely within a zone of zero-thickness which corresponds to the height of the diffusion flame. The flame height is larger at the same x and increases faster with x for HR than for NHR, which is shown by the configuration of the flame sheet for the two cases in Fig. 8. By comparison of profiles at $x=0.38$, the fuel mass fraction is nonzero only for HR, indicating that the fuel mass is transferred upstream of the burner and the chemical reaction occurs there. This proves that the boundary layer approximation is invalid, at least near the leading edge. The diffusion thickness of the fuel, defined as the distance along the y-direction within which the profile has a nonzero gradient, is significantly larger for HR than for NHR. Vertically away from the surface of the burner, the fuel mass fraction tends to immediately decrease for HR, while remaining almost unity for a fair distance for NHR. A possible reason for this is that, at the side of the fuel below the flame sheet for HR, negative velocity in the y-direction exists and mass transfer of the fuel towards the flame sheet is hindered. However, mass transfer is enhanced for NHR because the velocity in the y-direction remains positive in the fuel side of the flame sheet. According to this, it is expected that in some cases of flows with finite-rate exothermic reactions, reaction rates decrease with increasing in amounts of heat release because mass transfer of reactants toward the reaction zone is hindered, in spite of possible increases in diffusion coefficients when temperature increases. In fact, this tendency has been found and reported in the literature, but its mechanism is not yet well understood. From Fig. 8 it can be noted that the leading edge of the flame is anchored upstream of the burner for HR, while it is just on the leading edge of the burner for NHR; the flame sheet is shifted further away from the wall for HR than for NHR.

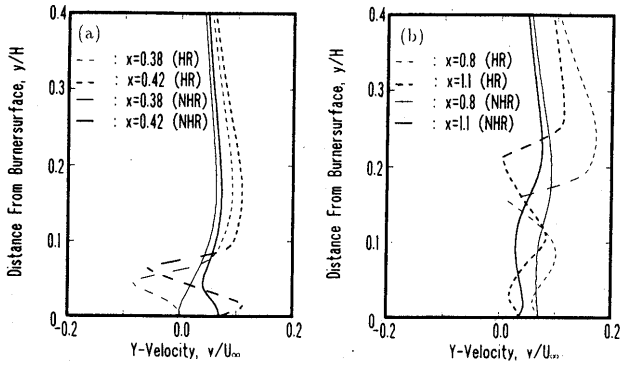

Fig. 6 Profiles of the velocity in the y-direction

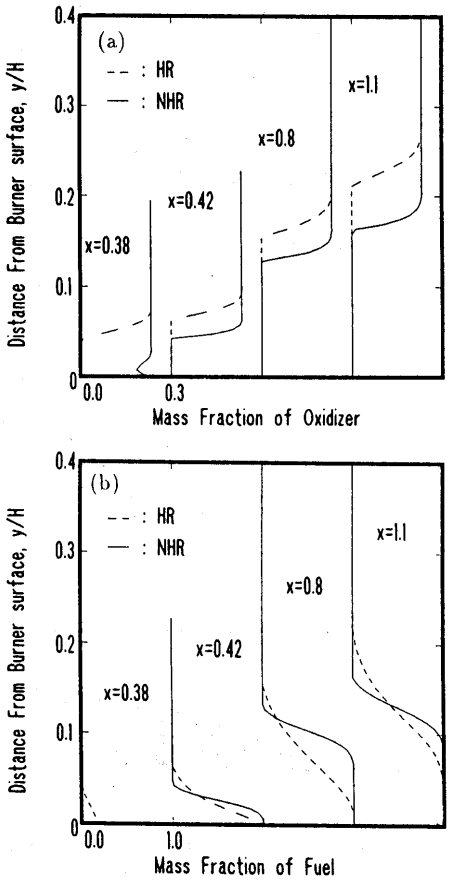

Fig. 7 Profiles of mass fractions of the oxidizer and fuel along the y-direction

3.2 Effect of main stream velocity

The effect of main stream velocity, i.e., the Reynolds number of the main stream, is analyzed by using the results for HR at three different Reynolds numbers. Profiles of the velocity in the x-direction along y are depicted in Fig. 9 at $x=0.403, 0.8, 1.1$. In

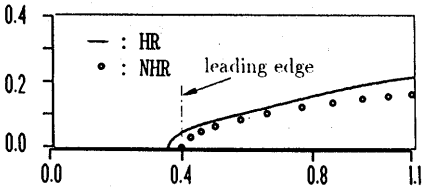

Fig. 8 Flame sheets for two cases

the vicinity of the burner surface, velocity increases faster at higher Re at all three positions. At the low Reynolds number $Re=3117$ near the front end of the burner at $x=0.403$, the profile has a negative gradient, indicating the presence of a separating and recirculating zone in the flow. Recirculating flows are also found for HRe and MRe, but there exist differences in the size and location of the recirculating zone among the three Re, e.g., the zone is expanded when Re decreases. With the decrease in Re, the velocity profile is distorted and the velocity overshoot becomes apparent, having maxima of 1.16, 1.37, 1.69 respectively for HRe, MRe and LRe, which shows qualitatively agreement with experimental measurements reported by Hirano et al.[2),3)] and by Mori et al.[6]. The distortion in the velocity induced by the baroclinic torque and the thermal expansion is closely connected with an unstable flame structure, as observed in the direct and schileren photographs of the flames in experiments under the same conditions[12]. In the experiments, the flame is observed to experience different shapes when Re increases. At low Re the flame zone shows a large-scale vibration downstream of the burner, and at high Re the flame is blown off the leading edge of the burner. The former is thought to be produced in the presence of the counter-rotating vortices along the flame sheet, and the latter is caused by the coupling of chemistry and fluid dynamics. A high velocity of the main stream results in insufficient residence time for the reactants to mix and react near the front of the burner, thus, the flame can not be stabilized there and is blown downstream.

Profiles of fuel mass fractions in the y-direction are given in Fig. 10 at three values of x. At low Re the mass fraction of fuel has a larger diffusion thickness, which tends to decrease as Re increases. Downstream the thickness increases in all three cases. From the configuration of flame sheets shown in Fig. 11 at the three values of Re, flame height increases and the leading edge of the flame anchors more upstream of the burner as Re decreases. This is closely related to the mass transfer of the fuel upstream due to the formation of a recirculation flow there.

Contours of pressure and vorticity are shown in Fig. 12 for two Reynolds numbers, $Re=3117$ and 9352. Those at $Re=6234$ are shown in Fig. 5. With a

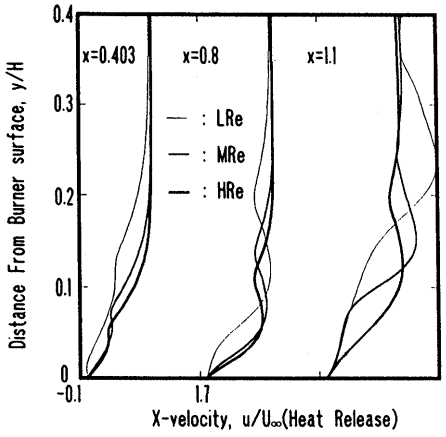

Fig. 9 Profiles of the velocity in the x-direction

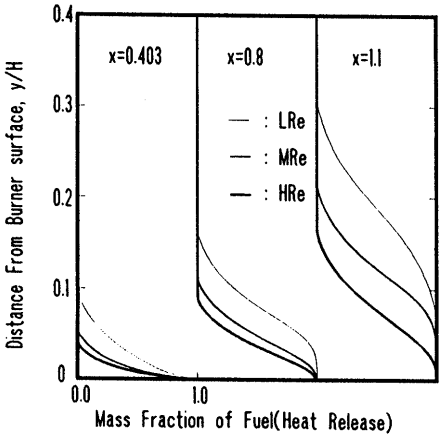

Fig. 10 Profiles of mass fraction of the fuel along the y-direction

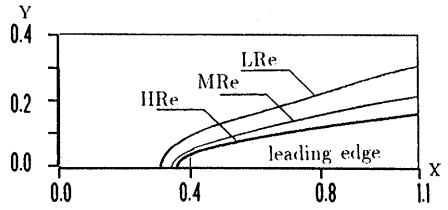

Fig. 11 Flame sheets at three Reynolds numbers

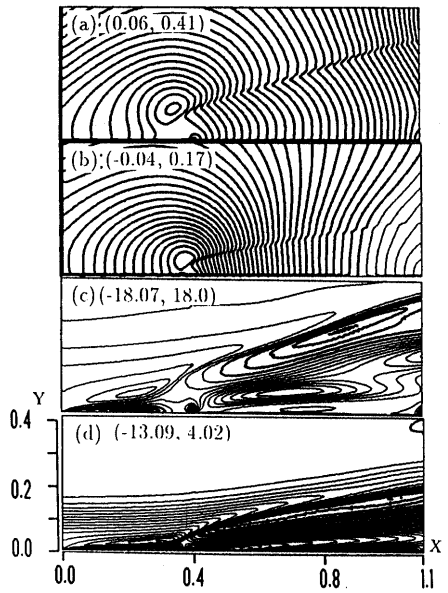

Fig. 12 Contours of pressure and vorticity torque for HR: (a) pressure for LRe, (b) pressure for HRe, (c) vorticity for LRe and (d) vorticity for HRe (data in brackets indicate maxima and minima of the contours)

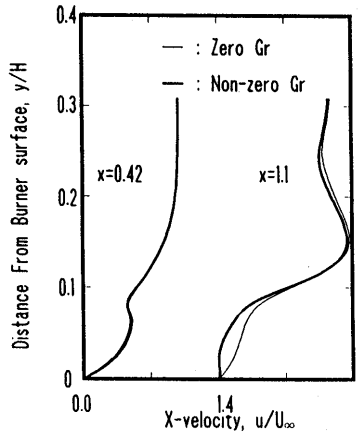

Fig. 13 Profiles of the velocity in the x-direction

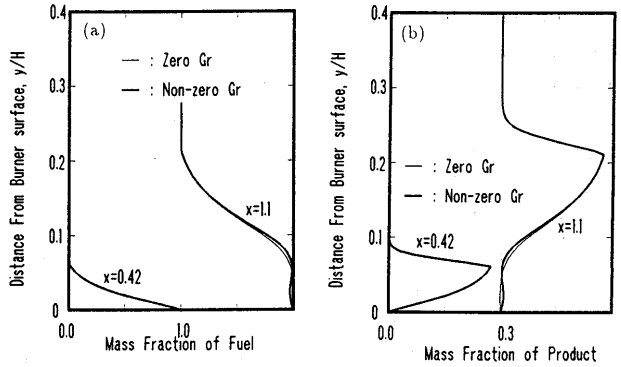

Fig. 14 Profiles of mass fractions of the (a) fuel and (b) product

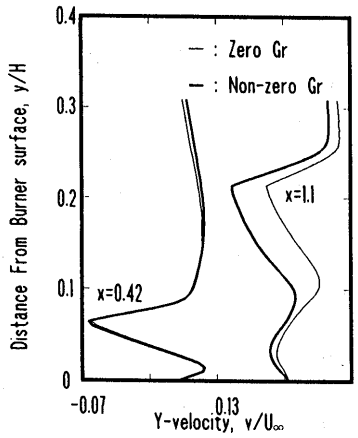

Fig. 15 Profiles of the velocity in the y-direction

decrease in Re, the high pressure zone moves both upstream and away from the wall, which causes the recirculation to move upstream. Especially at $Re=3117$, two local extrema in pressure are observed near the leading edge of the burner, and the pressure difference is the largest among the three cases. Similar to the vorticity pattern shown in Fig. 5, positive vorticity also predominates along the flame sheet in the two cases.

3.3 Effect of buoyancy

In general, chemically reacting boundary layer flows are affected by mixed convection: forced one and free one, which can be reflected by a dimensionless quantity $\eta=Gr/Re^2$. The term $\eta>1$ indicates predominantly a free convection flow, perturbed by a forced convection, and an η of unity corresponds to a flow in which both effects are comparable. In this case (Case 7), η is specified as 0.5, indicating a predominantly forced convection perturbed by free convection. The effect of buoyancy on the behavior of flow and flame has been examined in several cases and two are those of a zero and non-zero Grashof number (Gr) at $Re=6234$. Profiles of the velocity in the x-direction are depicted in Fig. 13 at $x=0.42$ and 1.1. The difference in the velocity profiles between the two cases is hard to see near the upstream part of the burner at $x=0.42$, but it is somewhat apparent in the vicinity of the wall at the rear end of the burner. The buoyancy makes a negligible contribution to the generation of the velocity overshoot because almost no variation is evident in magnitude and position of the overshoot. This observation shows the same trend as the results of West et al.[13] in their modeling effort. It was concluded that a striking similarity between flame spreading in a naturally induced flow compared with a forced flow exists and that the reason for the similarity is the comparability of the velocity distribution near the surface and leading edge of the flame. Profiles of mass fractions of the fuel and the product are given in Figs. 14(a) and 14(b) respectively, from which it can be seen that buoyancy causes minimal influence on the profiles, implying small change in the mass transfer of the reactants. Only in the rear of the burner does the direct effect of buoyancy appear in terms of the y-direction momentum, i.e., by the y-direction velocity, profiles of which are shown in Fig. 15. An obvious discrepancy is noted on the profile downstream of the burner ($x=1.1$), and a small augmentation in the velocity in the y-direction occurs, although the profile for the non-zero Gr case possesses a similar pattern to that for the zero Gr case.

4. Conclusions

A numerical simulation is carried out on a chemically reacting laminar boundary layer flow, and the generation of counter-rotating vortices along the flame sheet is investigated to clarify the mechanisms producing anomalies in velocity distribution and hydrodynamic instability. We conclude the following:

(1) For HR, a narrow strip zone with positive vorticity is observed along the flame sheet and is surrounded by predominantly negative vorticity. This indicates a series of counter-rotating vortices along the flame sheet. The movement and development of

these vortices may perturb and wrinkle the flame sheet if they become strong enough.

(2) In cases of exothermic reactions, a recirculating flow occurs near the front of the burner, which is responsible for the upstream movement of the leading flame. A high pressure zone and a velocity overshoot are obvious in all the cases. Mechanisms responsible for these are expected to involve the effects of the baroclinic torque and thermal expansion.

(3) With a decrease in Reynolds number, the velocity profile in the x-direction is distorted severely and the velocity overshoot becomes apparent; flame height increases, and its leading edge is anchored more upstream of the burner; a high pressure zone tends to move upward and results in a strong favorable pressure gradient.

(4) Buoyancy has a negligible contribution to the generation of the velocity overshoot and has little effect on the diffusion of chemical reactants over the burner, although it will act far downstream of the burner.

References

(1) Emmons, H., The Film Combustion of Liquid Fuel, Z. Angew. Math. Vol. 36 (1956), p. 60.

(2) Hirano, H. and Kanno, Y., Aerodynamic and Thermal Structures of the Laminar Boundary Layer over a Flat Plate with a Diffusion Flame, 14th Symp. (Intl.) on Combustion (1972), p. 391.

(3) Hirano, H. and Kinoshita, M., Gas Velocity and Temperature Profiles of a Diffusion Flame Stablized in the Stream over Liquid Fuel, 15th Symp. (Intl.) on Combustion (1974), p. 379.

(4) Zhou, L. and Fernandez-Pello, A.C., Solid Fuel Combustion in a Forced, Turbulent, Flat Plate: the Effect of Buoyancy, 24th Symp. (Intl.) on Combustion (1992), p. 1721.

(5) Lavid, M. and Berlad, A.L., Gravitational Effects on Chemically Reacting Laminar Boundary Layer Flows over a Horizontal Flat Plate, 16th Symp. (Intl.) on Combustion (1976), p. 1557.

(6) Mori, Y., Hijikata, K., Miyauchi, T. and Ikeda, H., Fundamental Investigation on Diffusion Flame of a Laminar Boundary Layer over a Liquid Fuel Surface, Trans. Jpn. Soc. Mech. Eng., Vol. 48 (1982), p. 1174.

(7) Trevino, G., Pressure Variations of a Steady Premixed Flame in a Boundary Layer Flow, 18th Symp. (Japan) on Combustion (1980), p. 85.

(8) Chen, C-H. and T'ien, J.S., Diffusion Flame Stabilization at the Leading Edge of a Fuel Plate, Combust. Sci. and Tech., Vol. 50 (1986), p. 283.

(9) Strehlow, R.A., Combustion Fundamentals, (1984), p. 54, McGraw-Hill, New York.

(10) Lee, S.T. and T'ien, J.S., A Numerical Analysis of Flame Flashback in Premixed Laminar System, Combustion and Flame, Vol. 48 (1982), p. 273.

(11) McMurtry, P.A., Riley, J.J. and Metcalfe, R.W., Effect of Heat Release on the Large-Scale Structures in Turbulent Mixing Layers, J. Fluid Mech., Vol. 199 (1989), p. 297.

(12) Katoh, H., Wang, X., Yoshihashi, T. and Ohyagi, S., Stabilization of a Diffusion Flame Behind Obstacles, Presented to the 4th ASME-JSME Thermal Engineering Conference, (1995).

(13) West, J., Bhattacharjee, S. and Altenkirch, R. A., A Comparison of the Roles Played by Natural and Forced Convection in Opposed-flow Flame Spreading, Combust. Sci. Tech. (83) 1992, p. 233.